

Direct probe of magnetic field effects on phonons by ultrasound propagation in a quasi-two-dimensional honeycomb magnet $\text{Na}_2\text{Co}_2\text{TeO}_6$

Xiaochen Hong^{1,2,3,*}, Maximilian Schiffer², Beat Valentin Schwarze⁴, Marc Uhlarz⁴, Xianghong Jin⁵, Weiliang Yao⁵, Lukas Janssen⁶, Sergei Zherlitsyn⁴, Bernd Büchner^{3,7}, Yuan Li^{5,8}, Young Sun¹ and Christian Hess^{2,3,†}

¹*Department of Applied Physics and Center of Quantum Materials and Devices,
Chongqing University, 401331 Chongqing, China*

²*Fakultät für Mathematik und Naturwissenschaften,*

Bergische Universität Wuppertal, 42097 Wuppertal, Germany

³*Leibniz-Institute for Solid State and Materials Research (IFW-Dresden), 01069 Dresden, Germany*

⁴*Hochfeld-Magnetlabor Dresden (HLD-EMFL) and Würzburg-Dresden Cluster of Excellence ct.qmat,
Helmholtz-Zentrum Dresden-Rossendorf, 01328 Dresden, Germany*

⁵*International Center for Quantum Materials, School of Physics, Peking University, 100871 Beijing, China*

⁶*Institut für Theoretische Physik and Würzburg-Dresden Cluster of Excellence ct.qmat,
Technische Universität Dresden, 01062 Dresden, Germany*

⁷*Institute of Solid State and Materials Physics and Würzburg-Dresden Cluster of Excellence ct.qmat,
Technische Universität Dresden, 01062 Dresden, Germany*

⁸*Beijing National Laboratory for Condensed Matter Physics,
Institute of Physics, Chinese Academy of Sciences, 100190 Beijing, China*

(Dated: June 10, 2025)

We study the phonon behavior of a Co-based honeycomb frustrated magnet $\text{Na}_2\text{Co}_2\text{TeO}_6$ under magnetic field applied perpendicular to the honeycomb plane. The temperature and field dependence of the sound velocity and sound attenuation unveil prominent spin-lattice coupling in this material, promoting ultrasound as a sensitive probe for magnetic properties. An out-of-plane ferrimagnetic order is determined below the Néel temperature $T_N = 27$ K. A comprehensive analysis of our data further provides strong evidence for a triple-Q ground state of $\text{Na}_2\text{Co}_2\text{TeO}_6$. Furthermore, the ultrasound data underscore that the field impact on the thermal conductivity as recently reported is of pure phononic origin.

INTRODUCTION

Phonons, the quanta of lattice vibrations, are ubiquitous in solid-state systems. Beyond their classical manifestations in thermodynamics, transport properties, and structural stability, phonons can couple strongly to electronic and magnetic degrees of freedom through elastoelectric and elastomagnetic interactions, giving rise to a rich array of emergent phenomena, including conventional superconductivity. For quantum spin liquids (QSLs), most of which are good insulators, phonons can provide a unique window into their exotic quasiparticles by coupling to emergent magnetic excitations such as spinons, Majorana fermions, and emergent gauge fields [1–3].

It is fair to say that renewed attention to the quasi-two-dimensional cobalt systems was drawn by the proposal that Co-based honeycomb magnets might realize Kitaev QSL physics [4–6]. A wave of experiments have revealed many resemblances between $\text{Na}_2\text{Co}_2\text{TeO}_6$ (NCTO) and the leading Kitaev QSL candidate $\alpha\text{-RuCl}_3$ [7–14]. However, NCTO exhibits an out-of-plane ferrimagnetic order [7], which is incompatible with a pure Kitaev QSL ground

state. Furthermore, detailed theoretical calculations suggested that the Kitaev interaction, while present, is not the dominant term in NCTO's Hamiltonian [15]. These facts fuel the debates about whether the exotic thermal transport results reported in $\alpha\text{-RuCl}_3$, once regarded as signatures of QSL states, are just from phonons influenced by magnetic excitation [16–18]. Practically, extracting the putative charge-neutral electronic excitations of interest from a phonon background invokes comparison with a nonmagnetic reference compound or a power-law fitting of the $\kappa_{ph}(T)$ curves in a limited temperature range. Both of these procedures are tricky and proliferate the discrepancies in interpreting the data. In this context, it is important to get more detailed knowledge of the phonons in this material class.

Ultrasound measurements provide a powerful experimental tool for directly probing phonon behavior in solids [19]. By analyzing changes in the phase and amplitude of ultrasound waves after propagation through a sample, and by monitoring their dependence on temperature and magnetic field, this technique enables high-resolution detection of variations in the sound velocity $\Delta v/v$ and sound attenuation $\Delta\alpha$ [20]. This method has been extensively employed to study the phase diagrams of frustrated magnets [20, 21], which often host a plethora of magnetic transitions due to competing interactions. In particular, its application to spinel systems has demonstrated its effectiveness as a sensitive probe, capable of revealing sub-

*hongxc@cqu.edu.cn

†c.hess@uni-wuppertal.de

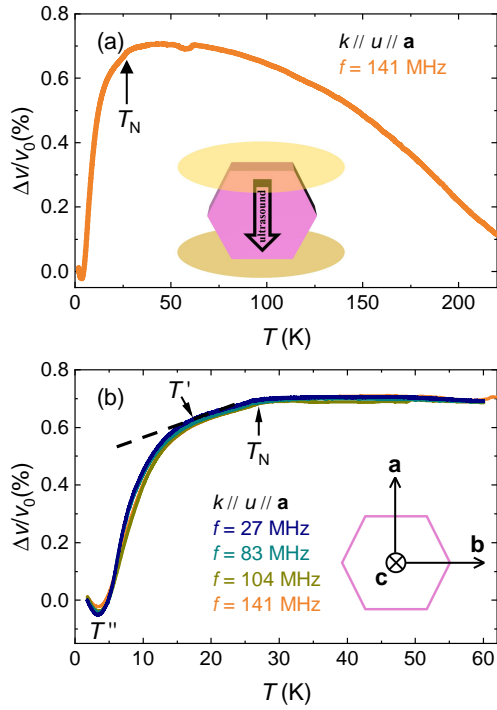


FIG. 1: (a) Representative temperature dependence of $\Delta v/v_0$, collected in the LA mode at the ultrasound frequency $f \approx 141$ MHz. (b) The low temperature data at different ultrasound frequencies. Three anomalies $T_N = 27$ K, $T' = 16$ K, and $T'' = 4$ K can be addressed. The cartoons illustrate the experimental geometry.

the changes in lattice and spin dynamics [22]. Recently, ultrasound measurements have also been implemented to explore the elusive Majorana fermion under an in-plane magnetic field in α - RuCl_3 [23, 24].

In this work, we focus on measuring the impact of out-of-plane ($\mathbf{B} // \mathbf{c}$) magnetic fields on the in-plane ultrasound properties of NCTO. Our results demonstrate that ultrasound serves as a sensitive probe of structural and magnetic transitions in NCTO. Very rich phenomena are revealed below its Néel temperature ($T_N = 27$ K). By analyzing our results, we confirm the existence of an out-of-plane ferrimagnetic order in NCTO and provide evidence supporting a triple-Q ground state [25, 26]. Furthermore, we explore the relationship between our ultrasound data and the reported thermal transport results under out-of-plane magnetic fields [11, 27], offering new insights into the interplay between lattice dynamics and magnetic excitations in this material and beyond.

EXPERIMENTAL METHOD

Single crystals of NCTO were prepared with a modified flux method [7]. Although the typical thickness of the as-grown crystals are about 0.1 mm, very few of

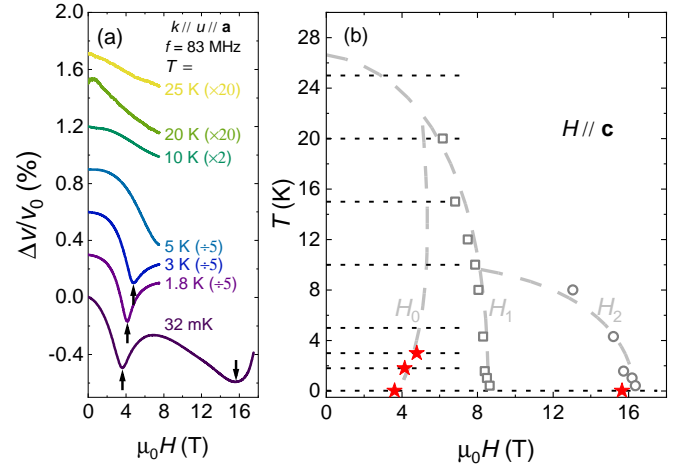


FIG. 2: (a) Field dependence of $\Delta v/v_0$ at different temperatures. The curves are shifted vertically for clarity. Note the different rescale factors for each curve. The black arrows indicate the dips in some curves. (b) The gray circles, squares, and dashed lines are phase boundaries of NCTO inferred from its magnetic susceptibility data [31]. The red stars are the positions of anomalies from Fig. 2(a). We follow the notation for the critical fields H_1 and H_2 from Ref. [31]. Although there is a clear line below H_1 in the contour plot of dM/dH data, it was not labeled as a critical field in Ref. [31]. Nevertheless, an electron spin resonance (ESR) work identified it also as a phase transition [32]. Thus we use H_0 to name this line. The dashed black lines indicate the parameter space reached in Fig. 2(a).

them can be thicker, preferred by an ultrasound experiment [7]. Three of the thickest crystals, all with a thickness of 0.4 ± 0.05 mm, were selected from different batches for this work. NCTO has a hexagonal crystal structure (space group $P6_322$) [28]. The ultrasound propagation direction with the wave vector k was set along the crystallographic zigzag \mathbf{a} -direction (perpendicular to a Co-Co bond in the honeycomb plane, see the insets of Fig. 1) for simplicity. The polarization of the acoustic wave (u) was along \mathbf{a} , \mathbf{b} or \mathbf{c} crystallographic directions depending on the studied acoustic mode. The direction \mathbf{b} is along Co-Co bond within the honeycomb plane. The surfaces to which the transducers would be attached were carefully polished against ultra-fine grade abrasive papers.

Ultrasound measurements were performed using a pulse-echo phase-sensitive detection technique [20]. To generate and detect ultrasonic signals in the frequency range 20–150 MHz, a pair of LiNbO_3 ultrasound transducers (36° Y-cut for the longitudinal and 41° X-cut for the transverse waves) were attached to both sides of the sample with a liquid polymer Thiokol LP-32. The experiments were carried out in a physical property measurement system (PPMS) from Quantum Design and a dilution refrigerator from Oxford Instruments, both equipped with a superconducting magnet.

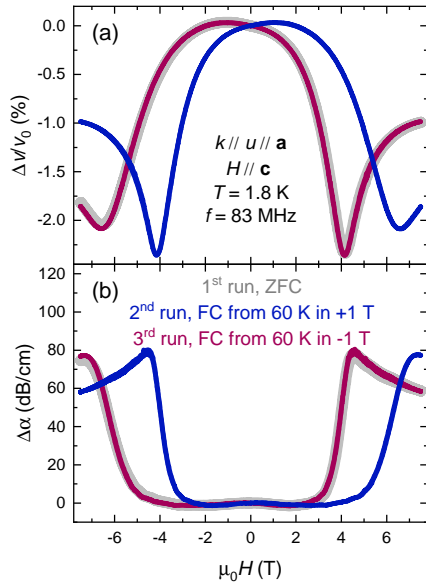


FIG. 3: Field dependence of (a) $\Delta v/v_0$ and (b) $\Delta\alpha$ at 1.8 K, measured in opposite field directions. The first field-sweep run was done after the sample was cooled in zero, or in small (< 14 mT) remanent field of our magnet. The second and third measurements were done after cooling in a finite field applied along opposite directions.

RESULTS AND DISCUSSION

The temperature dependence of the relative changes in the sound velocity $\Delta v/v_0$ for the longitudinal acoustic (LA) mode is shown in Fig. 1(a). The overall $\Delta v/v_0(T)$ curve reveals the lattice hardening upon cooling, and a softening appears below the magnetic transition temperature T_N . The data at low temperature is enlarged in Fig. 1(b), plotted together with results taken with various ultrasound frequencies, to check for a possible frequency dependence. All these curves overlap almost perfectly. Three anomalies can be reliably resolved, corresponding to the cascade of magnetic phase transitions below T_N reported in the literature [29, 30].

A set of field-dependent $\Delta v/v_0$ isotherms are presented in Fig. 2(a). Above 5 K, the $\Delta v/v_0(H)$ curves show moderate lattice softening in field without additional features up to 7.5 T. The amplitude of changes in $\Delta v/v_0(H)$ increases considerably upon cooling. A clear dip in $\Delta v/v_0(H)$ can be resolved at 3 K. This dip gradually shifts to a lower field at lower temperatures. At the lowest temperature of 32 mK another broader dip at round 16 T was detected. These features are summarized in Fig. 2(b) in the phase diagram of NCTO for an out-of-plane magnetic field, together with the transitions observed in the magnetic susceptibility [31]. While all the ultrasound anomalies can find their correspondence in magnetization, some magnetic transitions leave no detectable fingerprint in our ultrasound data. This fact

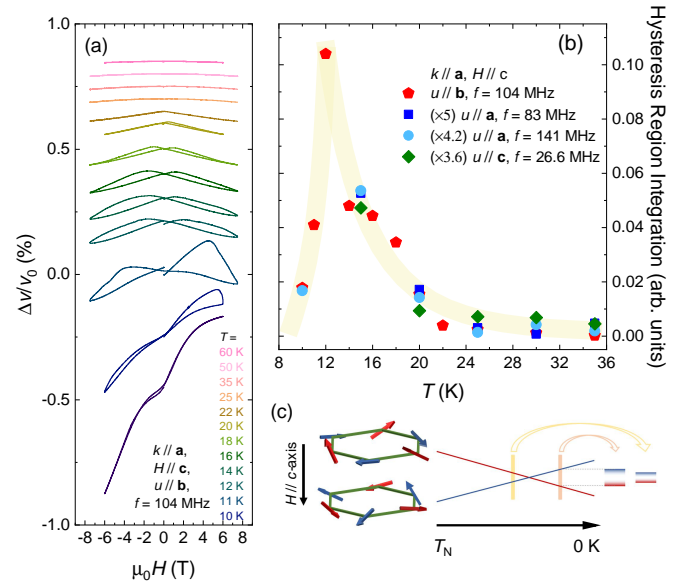


FIG. 4: (a) $\Delta v/v_0(H)$ isotherms measured in NCTO in opposite field directions. The curves are shifted vertically for clarity. (b) The temperature dependence of the integrated hysteric region of $\Delta v/v_0(H)$ isotherms. The data integrated up to 7.5 T from different experimental setting are rescaled to show a common temperature behavior. The yellow stripe is a guide to the eye. (c) Schematic diagram of the temperature and magnetic field effects on the out-of-plane magnetic components of two sub-lattices (red and blue arrows) with opposite sign and different magnitude, resides on a representative hexagon. Around the temperature at which the the energy of the opposite configurations in magnetic field is reversed, magnetic flipping is more likely to be promoted.

means that the acoustic modes in NCTO are selectively coupled to the spins. For the studied acoustic modes, the magnetoelastic coupling can be very small at some phase transitions in NCTO.

Recently, there have been some debates on whether the magnetic ground state of NCTO is an unusual triple-Q state or the conventional multi-domain zigzag order [26, 28, 33–35]. To shed more light on this issue, we investigated field dependence of $\Delta v/v_0$ and $\Delta\alpha$ under different cooling conditions (Fig. 3). We observe a very clear field-asymmetry depending on the cooling conditions, and it can be switched by changing the field cooling process from above T_N . This is a clear evidence of an out-of-plane ferromagnetic moment. It is compatible with the reported out-of-plane ferrimagnetic behavior in NCTO [7]. There are two mechanisms proposed for the ferrimagnetism in NCTO, both invoking the canting of the in-plane magnetic moments. Some previous work suggested a triple-Q ground state in NCTO and several other Co-based quasi-2D honeycomb magnets [25, 26, 33, 34, 36]. Another scenario insists that many cobaltates manifest a zigzag ground state stabilized within an XXZ model [15, 28, 31, 35], and the

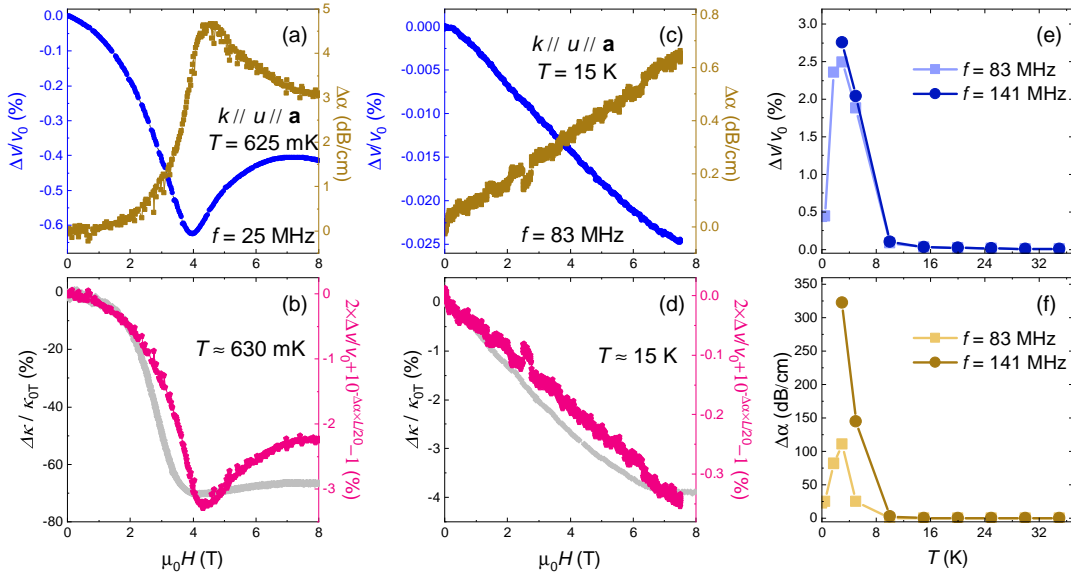


FIG. 5: Field dependence of $\Delta v/v_0$ and $\Delta \alpha$ at (a) 630 mK, and (c) 15 K. The corresponding estimates of the change of phonon conductivity (see text) are plotted in red in (b) and (d), respectively. Field dependence of the thermal conductivity κ at similar temperatures reported in the literature is also shown [11, 27]. Temperature dependence of maximum field-induced changes of (e) $\Delta v/v_0$ and (f) $\Delta \alpha$ measured with two different frequencies.

out-of-plane ferrimagnetism is due to unbalanced domains. Note that the zero-field-cooled (ZFC) $\Delta v/v_0(H)$ and $\Delta \alpha(H)$ data perfectly match the field-cooled (FC) data of the fully-switched states. It is unlikely that the alignment of domains can be made by a small remanent field. Hence, a more natural explanation is provided by a domain-free triple-Q ground state of NCTO.

To gain more insight, additional $\Delta v/v_0(H)$ results at elevated temperatures all the way up to above T_N are shown in Fig. 4(a). Obviously, the $\Delta v/v_0(H)$ curves are weakly field-suppressed and quite symmetric at temperatures higher than T_N . A butterfly-shaped hysteresis starts to grow at low temperatures. The hysteretic region and asymmetry are getting larger upon lowering the temperature. Finally, the hysteresis quickly shrinks, leaving very asymmetric $\Delta v/v_0(H)$ curves below about 12 K.

We use the integral of the enclosed region of the $\Delta v/v_0(H)$ curves to quantify the degree of hysteresis [Fig. 4(b)]. Data collected with different experimental settings were rescaled to fit into the same figure and to show a common temperature behavior for different acoustic modes. Notably, the hysteresis grows rapidly below T_N , reaches a maximum at around 12 K, and then drops quickly toward zero at lower temperature. As illustrated in Fig. 4(c), this behavior indicates that the energy difference between two magnetic configurations shrinks at around 12 K, not compatible with a XXZ ground state with domains developing below T_N . On the other hand, a recent Monte Carlo simulation work deduced a compensation point T_{cp} at roughly $T_N/2$ for a sign reversion of the residual magnetization out of the honeycomb plane,

if a triple-Q model is adopted for NCTO [36].

Finally, the effect of out-of-plane field on the thermal conductivity $\kappa(H)$ of NCTO are scrutinized with respect to the phonon properties. It is known that phonons dominate thermal transport in NCTO [27]. Since an out-of-plane magnetic field affects both the phonon speed and scattering rate, it may have dual effects on κ :

$$\kappa \propto Cvl = Cv^2\tau \propto \frac{Cv^2}{\Gamma}, \quad (1)$$

where l is the mean free path and τ is the relaxation time of phonons, which is inversely proportional to the scattering rate Γ . The phonon specific heat C is (to first order) field independent. The field-induced change of κ can be written as

$$\Delta \kappa \propto \frac{C(v_0 + \Delta v)^2}{\Gamma_0 + \Delta \Gamma} - \frac{Cv_0^2}{\Gamma_0}. \quad (2)$$

If considered to the lowest order, this can be approximated

$$\frac{\Delta \kappa}{\kappa} \approx 2 \times \frac{\Delta v}{v_0} - \frac{\Delta \Gamma}{\Gamma_0 + \Delta \Gamma}, \quad (3)$$

with the first and second term manifesting the contributions dominated by the field change of phonon speed and scattering rate, respectively. For pulse-echo ultrasound experiments, the damping term $\Delta \alpha$ is defined as

$$\Delta \alpha \equiv -\frac{20}{L} \log_{10} \frac{I}{I_0}, \quad (4)$$

where L is the effective sample length, and I is the ultrasound-signal amplitude [20, 23]. By assuming that

the scattering of phonons reduces the ultrasound signal and thermal transport in the same way, we get

$$\frac{\Gamma_0}{\Gamma} = \frac{\tau}{\tau_0} \propto \frac{I}{I_0} = 10^{-\Delta\alpha \times L/20}. \quad (5)$$

Substituting Eq. (5) into Eq. (3), we can write

$$\frac{\Delta\kappa}{\kappa} \approx 2 \times \frac{\Delta v}{v_0} + 10^{-\Delta\alpha \times L/20} - 1. \quad (6)$$

The estimated relative change in phonon thermal conductivity based on ultrasound data is shown in Fig. 5, by taking the sample thickness $L = 0.4$ mm in Eq. (6). The effect of the out-of-plane magnetic field on the thermal transport of NCTO at nearly the same temperature reported in the literature is also sketched for comparison [11, 27]. Their shape roughly matches, but the amplitude calculated from phonon data is underestimated by an order of magnitude or more. The reason might be that only one acoustic mode at a single frequency is considered in this work, while all phonon modes contribute to phonon thermal transport. As indicated in Fig. 5(f), the $\Delta\alpha$ term is strongly frequency dependent. Nevertheless, both $\Delta v/v$ and $\Delta\alpha$ peak at near 3 K, a temperature range that has not been investigated in previous work. We expect an impressively large field suppression of κ in this temperature range.

We are aware of the lowest temperature $\Delta v/v_0(H)$ curve reported in a recent ultrasound work on α - RuCl_3 features multiple humps and dips above its critical fields [23]. In the context of our results and discussion, our finding adds weight to the argument that the oscillatory structures in $\kappa(H)$ of α - RuCl_3 [37], initially attributed to some charge neutral magnetic excitations, might actually come from the strongly scattered phonon transport channels [18, 38].

SUMMARY

To summarize, using the ultrasound technique we studied the temperature and field induced transitions in NCTO. We observed strongly asymmetric and hysteretic features in the acoustic properties of NCTO in the magnetic field applied perpendicular to the honeycomb plane in opposite directions. Quantitative analyses of the hysteresis area unveiled a sharp maximum reached at around 12 K, with a strong suppression when the temperature is further lowered. This observation suggests the scenario with triple-Q ground state in NCTO rather than a zigzag ground state proposed from an XXZ model. Our ultrasound results are in line with the thermal transport data known from the literature [11, 27]. This fact strongly suggests that the intricate thermal transport features of NCTO at low temperatures have no direct contribution

from novel excitations beside phonons. Our results highlight that phonon effects must be considered very carefully when evaluating the experimental data of frustrated magnets.

ACKNOWLEDGMENTS

We thank J  r  my Sourd and Andreas Hauspurg for technical support. This work has been supported by the Deutsche Forschungsgemeinschaft (DFG) through Project No. 247310070 (SFB 1143), Project No. 390858490 (W  rzburg-Dresden Cluster of Excellence *ct.qmat*, EXC 2147), and Project No. 411750675 (Emmy Noether program, JA2306/4-1). This project has received funding from the European Research Council (ERC) under the European Unions-Horizon 2020 research and innovation programme (grant agreement No. 647276-MARS-ERC-2014-CoG). We acknowledge support of the HLD at HZDR, member of the European Magnetic Field Laboratory (EMFL). XCH acknowledge the start-up funding of Chongqing University.

-
- [1] L. Savary and L. Balents, *Quantum spin liquids: a review*, Rep. Prog. Phys. **80**, 016502 (2017).
 - [2] M. Ye, R. M. Fernandes, and N. B. Perkins, *Phonon dynamics in the Kitaev spin liquid*, Phys. Rev. Res. **2**, 033180 (2020).
 - [3] T. Oh and N. Nagaosa, *Phonon thermal Hall effect in Mott insulators via skew scattering by the scalar spin chirality*, Phys. Rev. X **15**, 011036 (2025).
 - [4] H. Liu and G. Khaliullin, *Pseudospin exchange interactions in d^7 cobalt compounds: Possible realization of the Kitaev model*, Phys. Rev. B **97**, 014407 (2018).
 - [5] R. Sano, Y. Kato, and Y. Motome, *Kitaev-Heisenberg Hamiltonian for high-spin d^7 Mott insulators*, Phys. Rev. B **97**, 014408 (2018).
 - [6] H. Liu, J. Chaloupka, and G. Khaliullin, *Kitaev spin liquid in 3d transition metal compounds*, Phys. Rev. Lett. **125**, 047201 (2020).
 - [7] W. Yao and Y. Li, *Ferrimagnetism and anisotropic phase tunability by magnetic fields in $\text{Na}_2\text{Co}_2\text{TeO}_6$* , Phys. Rev. B **101**, 085120 (2020).
 - [8] G. Lin, J. Jeong, C. Kim, Y. Wang, Q. Huang, T. Masuda, S. Asai, S. Itoh, G. G  nther, M. Russina, Z. Lu, J. Sheng, L. Wang, J. Wang, G. Wang, Q. Ren, C. Xi, W. Tong, L. Ling, Z. Liu, L. Wu, J. Mei, Z. Qu, H. Zhou, X. Wang, J.-G. Park, Y. Wan, and J. Ma, *Field-induced quantum spin disordered state in spin-1/2 honeycomb magnet $\text{Na}_2\text{Co}_2\text{TeO}_6$* , Nat. Commun. **12**, 5559 (2021).
 - [9] X. Hong, M. Gillig, R. Hentrich, W. Yao, V. Kocsis, A. R. Witte, T. Schreiner, D. Baumann, N. P  rez, A. U. B. Wolter, Y. Li, B. B  chner, and C. Hess, *Strongly scattered phonon heat transport of the candidate Kitaev material $\text{Na}_2\text{Co}_2\text{TeO}_6$* , Phys. Rev. B **104**, 144426 (2021).

- [10] A. L. Sanders, R. A. Mole, J. Liu, A. J. Brown, D. Yu, C. D. Ling, and S. Rachel, *Dominant Kitaev interactions in the honeycomb materials Na₃Co₂SbO₆ and Na₂Co₂TeO₆*, Phys. Rev. B **106**, 014413 (2022).
- [11] H. Yang, C. Kim, Y. Choi, J. H. Lee, G. Lin, J. Ma, M. Kratochvilova, P. Proschek, E.-G. Moon, K. H. Lee, Y. S. Oh, and J.-G. Park, *Significant thermal Hall effect in the cobalt Kitaev system*, Phys. Rev. B **106**, L081116 (2022).
- [12] M. Gillig, X. Hong, C. Wellm, V. Kataev, W. Yao, Y. Li, B. Büchner, and C. Hess, *Phononic-magnetic dichotomy of the thermal Hall effect in the Kitaev material Na₂Co₂TeO₆*, Phys. Rev. Res. **5**, 043110 (2023).
- [13] L. Chen, E. Lefrancois, A. Vallipuram, Q. Barthelemy, A. Ataei, W. Yao, Y. Li, and L. Taillefer, *Planar thermal Hall effect from phonons in a Kitaev candidate material*, Nat. Commun. **15**, 3513 (2024).
- [14] X.-G. Zhou, H. Li, C. Kim, A. Matsuo, K. Mehlaawat, K. Matsui, Z. Yang, A. Miyata, G. Su, K. Kindo, J.-G. Park, Y. Kohama, W. Li, and Y. H. Matsuda, *Emergent quantum disordered phase in Na₂Co₂TeO₆ under intermediate magnetic field along c axis*, preprint online, arXiv:2408.01957.
- [15] S. M. Winter, *Magnetic couplings in edge-sharing high-spin d⁷ compounds*, J. Phys. Mater. **5**, 045003 (2022).
- [16] R. Hentrich, A. U. B. Wolter, X. Zotos, W. Brenig, D. Nowak, A. Isaeva, Th. Doert, A. Banerjee, P. Lampen-Kelley, D. G. Mandrus, S. E. Nagler, J. Sears, Y.-J. Kim, B. Büchner, and C. Hess, *Unusual Phonon Heat Transport in α -RuCl₃: Strong Spin-Phonon Scattering and Field-Induced Spin Gap*, Phys. Rev. Lett. **120**, 117204 (2018).
- [17] E. Lefrancois, G. Grissonnanche, J. Baglo, P. Lampen-Kelley, J. Yan, C. Balz, D. Mandrus, S. E. Nagler, S. Kim, Y.-J. Kim, N. Doiron-Leyraud, and L. Taillefer, *Evidence of a Phonon Hall Effect in the Kitaev Spin Liquid Candidate α -RuCl₃*, Phys. Rev. X **12**, 021025 (2022).
- [18] J. A. N. Bruin, R. R. Claus, Y. Matsumoto, J. Nuss, S. Laha, B. V. Lotsch, N. Kurita, H. Tanaka, and H. Takagi, *Origin of oscillatory structures in the magnetothermal conductivity of the putative Kitaev magnet α -RuCl₃*, APL Mater. **10**, 090703 (2022).
- [19] B. Lüthi, *Physical Acoustics in the Solid State*, (Springer, Berlin, 2005).
- [20] S. Zherlitsyn, S. Yasin, J. Wosnitza, A. A. Zvyagin, A. V. Andreev, and V. Tsurkan, *Spin-lattice effects in selected antiferromagnetic materials*, Low Temp. Phys. **40**, 123–133 (2014).
- [21] J. Wosnitza, S. A. Zvyagin, and S. Zherlitsyn, *Frustrated magnets in high magnetic fields—selected examples*, Rep. Prog. Phys. **79**, 074504 (2016).
- [22] V. Tsurkan, H.-A. K. von Nidda, J. Deisenhofer, P. Lunkenheimer, and A. Loidl, *On the complexity of spinels: Magnetic, electronic, and polar ground states*, Phys. Rep. **926**, 1–86 (2021).
- [23] A. Hauspurg, S. Zherlitsyn, T. Helm, V. Felea, J. Wosnitza, V. Tsurkan, K.-Y. Choi, S.-H. Do, M. Ye, W. Brenig, and N. B. Perkins, *Fractionalized excitations probed by ultrasound*, Phys. Rev. B **109**, 144415 (2024).
- [24] A. Hauspurg, S. Singh, T. Yanagisawa, V. Tsurkan, J. Wosnitza, W. Brenig, N. B. Perkins, and S. Zherlitsyn, *Spin-strain interactions under hydrostatic pressure in α -RuCl₃*, preprint online, arXiv:2503.04656.
- [25] W. G. F. Krüger, W. Chen, X. Jin, Y. Li, and L. Janssen, *Triple-q order in Na₂Co₂TeO₆ from proximity to hidden-SU(2) symmetric point*, Phys. Rev. Lett. **131**, 146702 (2023).
- [26] W. Chen, X. Li, Z. Hu, Z. Hu, L. Yue, R. Sutarto, F. He, K. Iida, K. Kamazawa, W. Yu, X. Lin, and Y. Li, *Spin-orbit phase behavior of Na₂Co₂TeO₆ at low temperatures*, Phys. Rev. B **103**, L180404 (2021).
- [27] X. Hong, M. Gillig, W. Yao, L. Janssen, V. Kocsis, S. Gass, Y. Li, A. U. B. Wolter, B. Büchner, and C. Hess, *Phonon thermal transport shaped by strong spin-phonon scattering in a Kitaev material Na₂Co₂TeO₆*, npj Quantum Mater. **9**, 18 (2024).
- [28] S. Zhang, S. Lee, A. J. Woods, W. K. Peria, S. M. Thomas, R. Movshovich, E. Brosha, Q. Huang, H. Zhou, V. S. Zapf, and M. Lee, *Electronic and magnetic phase diagrams of the Kitaev quantum spin liquid candidate*, Phys. Rev. B **108**, 064421 (2023).
- [29] E. Lefrancois, M. Songvilay, J. Robert, G. Nataf, E. Jordan, L. Chaix, C. V. Colin, P. Lejay, A. Hadj-Azzem, R. Ballou, and V. Simonet, *Magnetic properties of the honeycomb oxide Na₂Co₂TeO₆*, Phys. Rev. B **94**, 214416 (2016).
- [30] A. K. Bera, S. M. Yusuf, A. Kumar, and C. Ritter, *Zigzag antiferromagnetic ground state with anisotropic correlation lengths in the quasi-two-dimensional honeycomb lattice compound*, Phys. Rev. B **95**, 094424 (2017).
- [31] S. Zhang, S. Lee, E. Brosha, Q. Huang, H. Zhou, V. S. Zapf, and M. Lee, *Out-of-plane magnetic phase diagram of the Kitaev quantum magnet Na₂Co₂TeO₆*, Phys. Rev. B **110**, 144431 (2024).
- [32] A. K. Bera, S. M. Yusuf, F. Orlandi, P. Manuel, L. Bhaskaran, and S. A. Zvyagin, *Field-induced phase transitions and anisotropic magnetic properties of the Kitaev-Heisenberg compound Na₂Co₂TeO₆*, Phys. Rev. B **108**, 214419 (2023).
- [33] W. Yao, Y. Zhao, Y. Qiu, C. Balz, J. R. Stewart, J. W. Lynn, and Y. Li, *Magnetic ground state of the Kitaev Na₂Co₂TeO₆ spin liquid candidate*, Phys. Rev. Res. **5**, L022045 (2023).
- [34] X. Jin, M. Geng, F. Orlandi, D. Khalyavin, P. Manuel, Y. Liu, and Yuan Li, *Robust triple-q magnetic order with trainable spin vorticity in Na₂Co₂TeO₆*, preprint online, arXiv:2501.07843.
- [35] C. Dhanasekhar, M. Jawale, R. Kumar, D. C. Kakarla, S. Mahapatra, M. M. C. Chou, A. Sundaresan, H. D. Yang, A. V. Mahajan, *Susceptibility anisotropy and absence of ferroelectric order in the Kitaev spin liquid candidate Na₂Co₂TeO₆*, preprint online, arXiv:2502.01580.
- [36] N. Francini and L. Janssen, *Ferrimagnetism from triple-q order in Na₂Co₂TeO₆*, Phys. Rev. B **110**, 235118 (2024).
- [37] P. Czajka, T. Gao, M. Hirschberger, P. Lampen-Kelley, A. Banerjee, J. Yan, D. G. Mandrus, S. E. Nagler, and N. P. Ong, *Oscillations of the thermal conductivity in the spin-liquid state of α -RuCl₃*, Nat. Phys. **17**, 915–919 (2021).
- [38] E. Lefrancois, J. Baglo, Q. Barthelemy, S. Kim, Y.-J. Kim, and L. Taillefer, *Oscillations in the magnetothermal conductivity of α -RuCl₃: evidence of transition anomalies*, Phys. Rev. B **107**, 064408 (2023).